

Topological inheritance in half-SSH Hubbard models

Suman Mondal¹, Sebastian Greschner², Luis Santos³ and Tapan Mishra¹

¹*Department of Physics, Indian Institute of Technology, Guwahati-781039, India*

²*Department of Quantum Matter Physics, University of Geneva, 1211 Geneva, Switzerland and*

³*Institute for Theoretical Physics, Leibniz University of Hannover, Hannover, Germany*

(Dated: August 18, 2020)

The interplay between interparticle interactions and topological features may result in unusual phenomena. Interestingly, interactions may induce topological features in an originally trivial system, as we illustrate for the case of a one-dimensional two-component Hubbard model in which one component is subjected to Su-Schrieffer-Heeger (SSH) dimerization, whereas the other one is not. We show that due to inter-component interactions the topological properties of one component are induced in the originally trivial one. Although for large interactions topological inheritance may be readily explained by on-site pairing, we show that the threshold for full inheritance occurs at weak interactions, for which the components are not yet paired. We illustrate this inheritance by discussing both bulk and edge properties, as well as dynamical observables as mean chiral displacement and charge pumping.

Symmetry protected topological (SPT) phase transitions are a class of phase transitions which do not come under the well-known Landau-Ginzburg paradigm associated with symmetry breaking. After the seminal observation of the fractional quantum Hall effect in condensed-matter systems [1–6], research on SPT phases in disparate systems ranging from exotic materials, ultracold neutral atoms, trapped ions, or photonic systems has earned enormous attention in recent years [7–14].

One of the simplest models exhibiting an SPT phase transition is the Su-Schrieffer-Heeger (SSH) model, which was first discussed in the context of solitons in polyacetylene [15]. The SSH model is a two-band one-dimensional tight-binding model with dimerized hoppings, which exhibits a topologically trivial to non-trivial transition through a gapless point. The non-trivial phase possesses zero-energy edge modes and a non-zero quantized Zak phase [16]. The non-interacting SSH model has been extensively analysed as a paradigmatic model to understand topological phenomena in various systems [17–23]. It has been recently implemented in quantum gas and photonic experiments [14, 24–27] and, in particular, Thouless topological charge pumping [28] has been observed [29–35]. Interactions lead to exciting new physics due to the competing interplay of correlation effects, particle statistics, and lattice topology, as recently discussed theoretically for both Bose- [23, 36, 37] and Fermi-Hubbard models [38–43].

In this paper, we show how, due to interactions, a topological system may induce topological features in a non-topological one. In particular, we consider a two-component system, in which one of the components experiences dimerized hopping, and hence an SSH model, whereas the other presents non-dimerized hopping, and would be hence topologically trivial if considered alone. We show that a finite interaction (attractive or repulsive) coupling the two species maps topological properties into the a-priori non-topological component, resulting in the

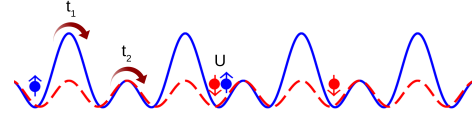


FIG. 1. (Color online) Two different species $\{\uparrow, \downarrow\}$ in the Model (1). Whereas \uparrow experiences SSH hopping dimerization with $t_1 \neq t_2$, \downarrow is in a homogeneous lattice with uniform hopping amplitude t . The inter-component interaction is denoted as U .

formation of strongly-correlated edge pairs.

Model.— We consider two Bose components $\{\uparrow, \downarrow\}$, such that \uparrow experiences SSH dimerization, whereas \downarrow is not dimerized. The interacting many-body system is described by the model:

$$\mathcal{H} = -t_1 \sum_{i \in \text{odd}} (c_{i\uparrow}^\dagger c_{i+1\uparrow} + \text{H.c.}) - t_2 \sum_{i \in \text{even}} (c_{i\uparrow}^\dagger c_{i+1\uparrow} + \text{H.c.}) - t \sum_i (c_{i\downarrow}^\dagger c_{i+1\downarrow} + \text{H.c.}) + U \sum_i n_{i\uparrow} n_{i\downarrow} \quad (1)$$

where $c_{i\sigma}^\dagger$ and $c_{i\sigma}$ are the creation and annihilation operators for $\sigma = \uparrow, \downarrow$ at site i , $n_{i\sigma} = c_{i\sigma}^\dagger c_{i\sigma}$ are the number operators, t_1 and t_2 are the tunneling rates of \uparrow from odd and even sites, respectively, t is the hopping rate of \downarrow , and U characterizes the inter-component interaction. We consider the hard-core constraint, $n_{\uparrow, \downarrow} \leq 1$. Note that model (1) can be mapped to a Fermi mixture, which presents the same spectrum and diagonal correlations.

In absence of interactions ($U = 0$) model (1) reduces to two uncoupled models, an SSH model for \uparrow , and a trivial Hubbard model for \downarrow . The quantized Zak phase of \uparrow is zero for $t_1 > t_2$ (trivial phase) and π for $t_1 < t_2$ (topological phase). While the bulk remains gapped for both phases, only the latter possesses zero energy edge modes. In our density matrix renormalization group (DMRG) calculations below, we consider half-filling, in which the number of particles in both components $N_{\uparrow, \downarrow} = L/2$, for

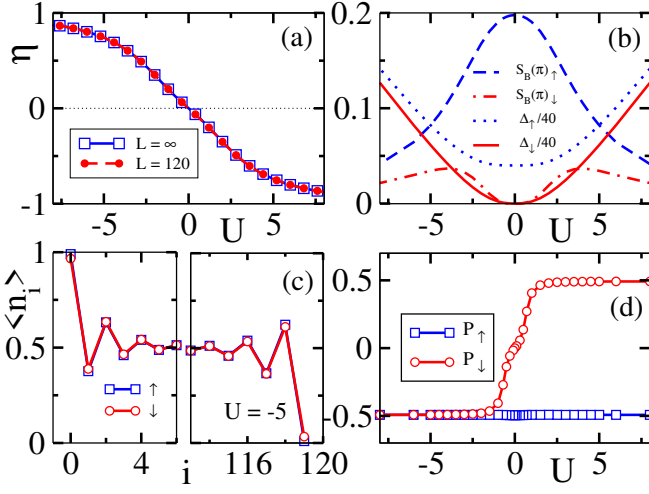


FIG. 2. (Color online) (a) Pairing η as a function of U ; (b) Bulk gaps Δ_σ (blue dotted and red continuous), and dimer structure factors $S_{D\sigma}(\pi)$ (blue dashed and red dot-dashed) for \uparrow and \downarrow components, respectively, as a function of U . The observables are extrapolated to $L \rightarrow \infty$ using our DMRG results for system sizes of length $L = 40, 60, 80, 100$ and 120 ; (c) Edge states for both component for $U = -5$ for a system with $L = 120$; (d) Polarization P_σ for \uparrow (blue squares) and \downarrow (red circles) as a function of U , obtained for $L = 120$.

a lattice with L sites. We set $t_2 = t = 1$ as energy unit, and fix $t_1 = 0.2$, within the non-trivial regime for \uparrow .

Pairing.— For a sufficiently strong $U < 0$ (> 0) a particle of one component pairs on-site with a particle (hole) of the other. Pairing is best monitored by $\eta = \frac{t}{L} \sum_i (\langle n_{i\uparrow} n_{i\downarrow} \rangle - \frac{1}{4})$, see Fig. 2(a). For large-enough $|U| > 8$, $|\eta| \simeq 1$ indicating strongly localized on-site pairing. For strong particle-particle pairing (particle-hole pairing is treated analogously), the system is described by an effective SSH model for on-site hard-core pairs:

$$\mathcal{H} = \frac{2t_1 t}{U} \sum_{i \in \text{odd}} P_i^\dagger P_{i+1} + \frac{2t_2 t}{U} \sum_{i \in \text{even}} P_i^\dagger P_{i+1} + \text{H.c.}, \quad (2)$$

with $P_i = c_{i\uparrow} c_{i\downarrow}$. Model (2) is topological if the SSH model for \uparrow is topological. Hence, the pairs (and with them the second component) inherit the topology of the first component. Interestingly, as discussed below, much weaker pairing $\eta \ll 1$, and hence very moderate $|U|$, already suffices to induce full *topological inheritance*.

Induced bulk properties.— In absence of interactions, the \downarrow component is a gapless superfluid, whereas due to hopping dimerization the bulk of the \uparrow component is in a gapped dimer phase with a finite dimer structure factor, $S_{D\sigma}(k) = \frac{1}{L^2} \sum_{i,j} e^{ikr} \langle D_{i\sigma} D_{j\sigma} \rangle$, with $D_{i\sigma} = c_{i\sigma}^\dagger c_{i+1\sigma} + \text{H.c.}$ The dotted blue (solid red) curve in Fig. 2(b) depicts the charge gap $\Delta_\sigma = E(L, N_\sigma + 1) + E(L, N_\sigma - 1) - 2E(L, N_\sigma)$ and dashed blue (dot-dashed red) curve depicts the dimer structure factor for both components. Strong pairing asymptotically results for large $|U|$ in an exact replication of the bulk properties

of the \uparrow component on the \downarrow component. Note, however, that any $U \neq 0$ (either repulsive or attractive) results in a finite bulk gap and dimer order in the spin- \downarrow component. Any finite interaction drives the bulk of the \downarrow component into a gapped dimer phase.

Induced edge states.— For $t_1 < t_2$ the \uparrow component is non-trivial, possessing doubly-degenerate edge modes. Sufficiently attractive (repulsive) interactions induced correlated (anti-correlated) edge states in \downarrow , see Fig. 2 (c). The inheritance of the edge states by the \downarrow component is best monitored by the polarization $P_\sigma = \frac{1}{L} \sum_{i=0}^L \langle \psi | (i - L/2) n_{i\sigma} | \psi \rangle$ for the ground state $|\psi\rangle$, which we depict in Fig. 2(d) for $L = 120$ for different values of U . Note that $P_\uparrow = -1/2$ due to the topological character of the \uparrow component. The \downarrow component shows maximally polarized edges, $|P_\downarrow| \simeq 1/2$, already for $|U| \sim 1$. Hence, the \downarrow component fully inherits the topological edge modes for values of $|U|$ well below those needed for strong pairing.

Mean chiral displacement.— Topological inheritance may be easily probed experimentally by monitoring the dynamical evolution after a quench. The mean-chiral displacement (MCD), recently utilized in the context of quantum random walk on a graph, can be utilized to measure the topological winding number in photonic and ultracold atomic systems [44–47]. The MCD is defined as $C_\sigma(\tilde{t}) = 2 \langle \Psi(\tilde{t}) | \Gamma_\sigma m_\sigma | \Psi(\tilde{t}) \rangle$, where Γ_σ and m_σ are the chiral and unit cell operators, respectively, and $|\Psi(\tilde{t})\rangle$ is the time-evolved state. The MCD displays an oscillatory behavior, but after a sufficiently large time its time averaging converges to the winding number ω [48].

We analyze the MCD by considering an initial state $|\Psi(0)\rangle = O |\Psi_{GS}\rangle$, with $|\Psi_{GS}\rangle$ the ground-state, and $O = c_{0\uparrow}^\dagger c_{0\downarrow}$ ($O = c_{0,\uparrow}^\dagger c_{0,\downarrow}$), i.e. pair annihilation (spin flip) at the central site, for $U < 0$ (> 0). Quantum walks from these initial states provide insights about the

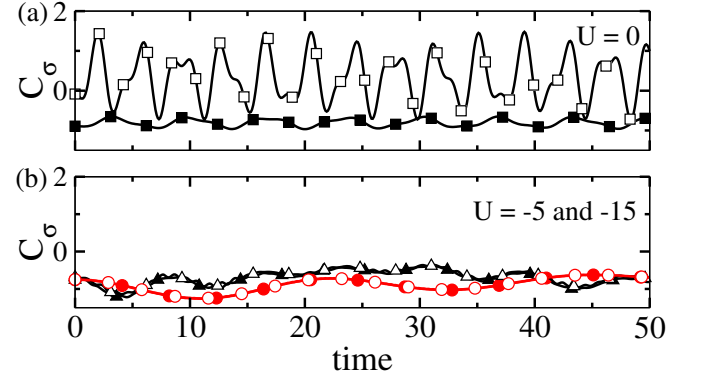


FIG. 3. (Color online) (a) MCD for a system with $L = 6$ for $U = 0$ for \uparrow (filled symbols) and \downarrow (hollow symbols); (b) Same for $U = -15$ (red circles) and $U = -5$ (black triangles). Here solid and empty symbols are corresponding to \uparrow and \downarrow respectively. For $|U| = 5(15)$ the MCD evolution curves are marked by symbol triangle(circle). In all cases we employ as initial state $|\Psi(0)\rangle = c_{0\uparrow} c_{0\downarrow} |\Psi_{GS}\rangle$.

charge and spin winding numbers, respectively. Figures 3 show our results of $C_\sigma(\bar{t})$, evaluated with the pair annihilation, for a system of size $L = 6$ with open boundary conditions. For $U_{\uparrow,\downarrow} = 0$ (Fig. 3(a)), $C_\uparrow(\bar{t})$ (filled squares) oscillates around the winding number -1 , as expected from the topological character of the \uparrow component. In contrast, $C_\downarrow(\bar{t})$ oscillates around zero (open squares), showing no topological behavior. When increasing the inter-component interaction, the MCD of both components becomes identical oscillating around the winding number (Fig. 3(b)) revealing the inheritance by the \downarrow component of the topological properties of the \uparrow component. Note that the deviations from the true winding numbers can be attributed to the finite size and interaction effects [49].

Thouless charge pumping.— Alternatively, topological inheritance may be dynamically probed by investigating Thouless charge pumping, i.e. the transport of quantized charge as a result of an adiabatic periodic modulation of the system parameters. We consider that only the \uparrow component is driven following a Rice-Mele (RM) model [50]

$$\mathcal{H}_\uparrow = - \sum_i \left[(t - (-1)^i \delta t \cos(2\tau)) c_{i,\uparrow}^\dagger c_{i+1,\uparrow} + \text{H.c.} \right] + \frac{\delta \Delta}{2} \sin(2\tau) \sum_i (-1)^i n_{i,\uparrow}. \quad (3)$$

where τ is a cyclic parameter used for the pumping protocol. The RM model reduces for $\tau = \pi/4$ and $3\pi/4$ to the SSH model [37, 51]. The pumping is best evaluated by monitoring the polarizations $P_\sigma(\tau) = \frac{1}{L} \sum_{i=0}^L \langle \psi(\tau) | (i - L/2) n_{i\sigma} | \psi(\tau) \rangle$. The total charge pumped during the cycle can be obtained by computing $Q_\sigma = \int_0^1 d\tau \partial_\tau P_\sigma(\tau)$. As expected, $P_\uparrow(\tau)$ (Fig. 4(a)) shows the robust pumping of one particle, indicating the existence of edge states. While no pumping occurs in \downarrow for $|U| = 0$, increasing $|U|$ leads to a finite pumping (Fig. 4(b)), despite the fact that only \uparrow is externally modulated. For $|U| \gtrsim 1$ the pumping of a full \downarrow particle marks the complete topological inheritance.

Inheritance threshold.— The previous results show that the \downarrow component fully inherits the topological properties of the \uparrow component (edge states, winding number, MCD, full-particle Thouless pumping) for inter-particle interactions beyond a given threshold. Such an inheritance threshold is not only revealed by the edge polarization (Fig. 2 (d)) and the change of character of the charge pumping (Figs. 4 (b) and (c)), but also by the analysis of the fidelity susceptibility, $\chi = \lim_{(U-U') \rightarrow 0} \frac{-2 \ln |\langle \psi_0(U) | \psi_0(U') \rangle|}{(U-U')^2}$. As shown in Fig. 4 (d), χ/L shows a clear maximum, that marks the inheritance threshold. Such a threshold approaches asymptotically $|U| \simeq 1.06$ for growing L . At the threshold, the pairing correlation $\eta \simeq 0.2$ (Fig. 2 (a)), and hence, remarkably, the on-set of full topological inheritance occurs when the components are not yet paired.

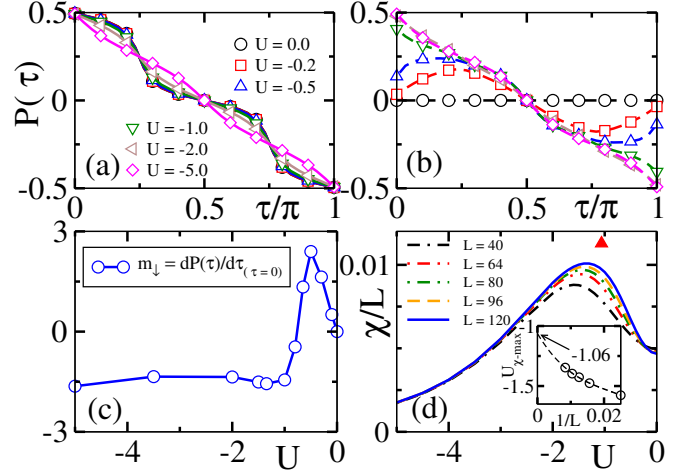


FIG. 4. (Color online) Polarizations $P_\uparrow(\tau)$ (a) and $P_\downarrow(\tau)$ (b) for different U values and $L = 120$; (c) Initial gradient $m_\downarrow = \frac{dP_\downarrow}{d\tau}(\tau=0)$ as a function of $U < 0$; (d) Fidelity susceptibility χ as a function of U for different L . The inset shows the extrapolation of the value U at which χ/L has a maximum. This value marks the onset of full topological inheritance. Here, the filled red triangle corresponds to the extrapolated position of the peak.

Conclusions.— Due to interactions, a topological system may induce topological features in a non-topological one, as we have illustrated for a Hubbard model in which a component experiences SSH dimerization and the other not. Although, for strong interactions topological inheritance may be readily understood from the formation of on-site localized inter-component pairs which experience an effective SSH model, we have shown that, interestingly, the threshold for full topological inheritance occurs for much weaker interactions, for which the two components are not yet paired.

A possible experimental realization of Model (1) may be achieved by employing two neighboring 1D lattices of hardcore dipolar bosons, which act like the two components $\{\uparrow, \downarrow\}$. Hopping dimerization in one of the chains can be introduced by using a secondary lattice on an already isolated ladder obtained using the primary lasers, as sketched in Fig. 5 (a). The Hubbard interaction can be simulated by aligning the dipoles in individual chains at the so-called magic angle, such that in-leg interactions vanish, and only inter-leg interactions are relevant.

Alternatively, state dependent optical lattices [52, 53] may allow for a direct experimental realization of Model (1). The latter may be extended to more than two components, for which topological inheritance may occur as well. As an example, Fig. 5 (b) shows our results for a three-component system (assuming $SU(3)$ -symmetric all-to-all interactions, $U_{SU(3)}$), in which only one component is topological. As for the two-component case, the trivial components fully inherit the topological properties for relatively weak interactions.

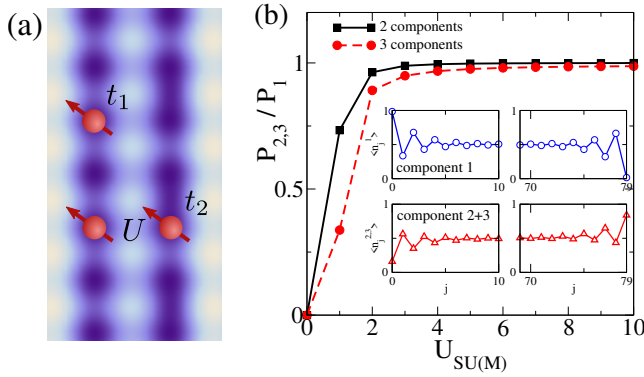


FIG. 5. (Color online) (a) Experimental scheme to realize Model (1) using two-leg optical ladder systems of hard-core dipolar bosons using dipolar particles (see text); (b) Induced polarization for a three-species system in a state-dependent super-lattice in the presence of on-site all-to-all (SU(3)-symmetric) interactions. The inset shows the replication of the edge state to the second and third species for $U_{SU(3)} = 6$.

The computational simulations were carried out using the Param-Ishan HPC facility at Indian Institute of Technology - Guwahati, India. S.G. acknowledges support by the Swiss National Science Foundation under Division II. T.M. acknowledges DST-SERB, India for the early career grant through Project No. ECR/2017/001069. L. S. acknowledges support of the Deutsche Forschungsgemeinschaft (DFG, German Research Foundation) under Germany's Excellence Strategy – EXC-2123 Quantum-Frontiers – 390837967.

[1] K. v. Klitzing, G. Dorda, and M. Pepper, *Phys. Rev. Lett.* **45**, 494 (1980).
[2] D. C. Tsui, H. L. Stormer, and A. C. Gossard, *Phys. Rev. Lett.* **48**, 1559 (1982).
[3] D. J. Thouless, M. Kohmoto, M. P. Nightingale, and M. den Nijs, *Phys. Rev. Lett.* **49**, 405 (1982).
[4] R. B. Laughlin, *Phys. Rev. Lett.* **50**, 1395 (1983).
[5] H. L. Stormer, A. Chang, D. C. Tsui, J. C. M. Hwang, A. C. Gossard, and W. Wiegmann, *Phys. Rev. Lett.* **50**, 1953 (1983).
[6] H. L. Stormer, *Rev. Mod. Phys.* **71**, 875 (1999).
[7] S. Rachel, *Reports on Progress in Physics* **81**, 116501 (2018).
[8] X.-L. Qi and S.-C. Zhang, *Rev. Mod. Phys.* **83**, 1057 (2011).
[9] M. Z. Hasan and C. L. Kane, *Rev. Mod. Phys.* **82**, 3045 (2010).
[10] N. R. Cooper, J. Dalibard, and I. B. Spielman, *Rev. Mod. Phys.* **91**, 015005 (2019).
[11] P. Nevado, S. Fernández-Lorenzo, and D. Porras, *Phys. Rev. Lett.* **119**, 210401 (2017).
[12] A. Mezzacapo, J. Casanova, L. Lamata, and E. Solano, *New Journal of Physics* **15**, 033005 (2013).

[13] K. Le Hur, L. Henriët, A. Petrescu, K. Plekhanov, G. Roux, and M. Schiró, *Comptes Rendus Physique* **17**, 808 (2016).
[14] T. Ozawa, H. M. Price, A. Amo, N. Goldman, M. Hafezi, L. Lu, M. C. Rechtsman, D. Schuster, J. Simon, O. Zilberberg, and I. Carusotto, *Rev. Mod. Phys.* **91**, 015006 (2019).
[15] W. P. Su, J. R. Schrieffer, and A. J. Heeger, *Phys. Rev. Lett.* **42**, 1698 (1979).
[16] J. Zak, *Phys. Rev. Lett.* **62**, 2747 (1989).
[17] M. Bello, G. Platero, J. I. Cirac, and A. González-Tudela, *Science Advances* **5** (2019), 10.1126/sciadv.aaw0297.
[18] G. Engelhardt, M. Benito, G. Platero, and T. Brandes, *Phys. Rev. Lett.* **118**, 197702 (2017).
[19] C. A. Downing and G. Weick, *Phys. Rev. B* **95**, 125426 (2017).
[20] H. Schomerus, *Opt. Lett.* **38**, 1912 (2013).
[21] R. Chaunsali, E. Kim, A. Thakkar, P. G. Kevrekidis, and J. Yang, *Phys. Rev. Lett.* **119**, 024301 (2017).
[22] C. L. Kane and T. C. Lubensky, *Nature Physics* **10**, 39 (2014).
[23] F. Grusdt, M. Hönig, and M. Fleischhauer, *Phys. Rev. Lett.* **110**, 260405 (2013).
[24] M. Atala, M. Aidelsburger, J. T. Barreiro, D. Abanin, T. Kitagawa, E. Demler, and I. Bloch, *Nature Physics* **9**, 795 (2013).
[25] E. J. Meier, F. A. An, and B. Gadway, *Nature Communications* **7**, 13986 (2016).
[26] N. Malkova, I. Hromada, X. Wang, G. Bryant, and Z. Chen, *Opt. Lett.* **34**, 1633 (2009).
[27] P. St-Jean, V. Goblot, E. Galopin, A. Lemaître, T. Ozawa, L. Le Gratiet, I. Sagnes, J. Bloch, and A. Amo, *Nature Photonics* **11**, 651 (2017).
[28] D. Thouless, *Phys. Rev. B* **27**, 6083 (1983).
[29] M. Lohse, C. Schweizer, O. Zilberberg, M. Aidelsburger, and I. Bloch, *Nature Physics* **12**, 350 (2015).
[30] S. Nakajima, T. Tomita, S. Taie, T. Ichinose, H. Ozawa, L. Wang, M. Troyer, and Y. Takahashi, *Nature Physics* **12**, 296 (2016).
[31] C. Schweizer, M. Lohse, R. Citro, and I. Bloch, *Phys. Rev. Lett.* **117**, 170405 (2016).
[32] M. Lohse, C. Schweizer, H. M. Price, O. Zilberberg, and I. Bloch, *Nature* **553**, 55 (2018).
[33] N. Goldman, J. Dalibard, A. Dauphin, F. Gerbier, M. Lewenstein, P. Zoller, and I. B. Spielman, *Proceedings of the National Academy of Sciences* **110**, 6736 (2013).
[34] M. Verbin, O. Zilberberg, Y. E. Kraus, Y. Lahini, and Y. Silberberg, *Phys. Rev. Lett.* **110**, 076403 (2013).
[35] M. Verbin, O. Zilberberg, Y. Lahini, Y. E. Kraus, and Y. Silberberg, *Phys. Rev. B* **91**, 064201 (2015).
[36] M. Di Liberto, A. Recati, I. Carusotto, and C. Menotti, *Phys. Rev. A* **94**, 062704 (2016).
[37] S. Greschner, S. Mondal, and T. Mishra, *Phys. Rev. A* **101**, 053630 (2020).
[38] T. Yoshida, I. Danshita, R. Peters, and N. Kawakami, *Phys. Rev. Lett.* **121**, 025301 (2018).
[39] L. Barbiero, L. Santos, and N. Goldman, *Phys. Rev. B* **97**, 201115 (2018).
[40] D. Wang, S. Xu, Y. Wang, and C. Wu, *Phys. Rev. B* **91**, 115118 (2015).
[41] B.-T. Ye, L.-Z. Mu, and H. Fan, *Phys. Rev. B* **94**, 165167 (2016).

- [42] P. Fromholz, G. Magnifico, V. Vitale, T. Mendes-Santos, and M. Dalmonte, *Phys. Rev. B* **101**, 085136 (2020).
- [43] X. Li, E. Zhao, and W. Vincent Liu, *Nature Communications* **4**, 1523 (2013).
- [44] E. J. Meier, F. A. An, A. Dauphin, M. Maffei, P. Massignan, T. L. Hughes, and B. Gadway, *Science* **362**, 929 (2018).
- [45] F. Cardano, A. D'Errico, A. Dauphin, M. Maffei, B. Piccirillo, C. de Lisio, G. De Filippis, V. Cataudella, E. Santamato, L. Marrucci, M. Lewenstein, and P. Massignan, *Nature Communications* **8**, 15516 (2017).
- [46] D. Xie, W. Gou, T. Xiao, B. Gadway, and B. Yan, *npj Quantum Information* **5**, 55 (2019).
- [47] D. Xie, T.-S. Deng, T. Xiao, W. Gou, T. Chen, W. Yi, and B. Yan, *Phys. Rev. Lett.* **124**, 050502 (2020).
- [48] We compute the winding number, $\omega = \int_0^\pi d\theta \langle \psi(\theta) | \partial_\theta \psi(\theta) \rangle$, of the ground state $|\psi\rangle$ of Model (1) with twisted boundary conditions $a_{i,\sigma} \rightarrow e^{i\theta_\sigma/L} a_i$.
The modified limit of integration and the two different twisting angles take care of the two different components [37]. Our exact numerical calculation for $L = 8$ shows that the winding number in the topological phase is appropriately captured as $\omega = 1$ for $|U| = 5$ with the choice of twist angle $\theta_\uparrow = \pm\theta_\downarrow$.
- [49] A. Haller, P. Massignan, and M. Rizzi, *Phys. Rev. Research* **2**, 033200 (2020).
- [50] M. Rice and E. Mele, *Phys. Rev. Lett.* **49**, 1455 (1982).
- [51] A. Hayward, C. Schweizer, M. Lohse, M. Aidelsburger, and F. Heidrich-Meisner, *Phys. Rev. B* **98**, 245148 (2018).
- [52] P. Soltan-Panahi, J. Struck, P. Hauke, A. Bick, W. Plenkers, G. Meineke, C. Becker, P. Windpassinger, M. Lewenstein, and K. Sengstock, *Nature Physics* **7**, 434 (2011).
- [53] B. Yang, H.-N. Dai, H. Sun, A. Reingruber, Z.-S. Yuan, and J.-W. Pan, *Phys. Rev. A* **96**, 011602 (2017).